RESEARCH ARTICLE Indian Journal of Animal Research, Volume 60 Issue 9: 1586-1595 (September 2026)

Promising Novel Anti-parasitic Drug Nitazoxanide/Mn Metal Complex with its Spectroscopic Characterization, Molecular Docking, DFT Analysis and Assessment of its *in vitro* Antioxidant Activity

Bander Albogami[1]

10.18805/IJAR.BF-2118

ABSTRACT

Background: Nitazoxanide (NITA) possesses a high potential activity against infections by various protozoa, but there is an urgent need for the development of new anti-pathogens with diverse metal chelation mechanisms to mitigate any possible side effects. Novel nitazoxanide/Mn complex (NITA/Mn) was chemically synthesized and fully characterized. Recent studies on metallic complexes present promising therapeutic agents against various diseases. As Manganese (Mn) acts as a critical antioxidant by serving as the essential metal cofactor for (MnSOD), the primary enzyme responsible for scavenging superoxide radicals in mitochondria, it was the target for chelation with NITA to synthesize a new potent antioxidant to alleviate any oxidative signs produced by NITA.

Methods: (NITA/Mn) complex was characterized using C,H, N and S elemental analysis, conductivity value, IR, UV, SEM and TEM, this paper explain the effect of NITA and NITA/Mn on oxidative stress via using antioxidant assays such as “ABTS, DPPH and metal chelation” assay with estimation of the novel synthesized metal complex stability *via* DFT analysis, The estimated percentages obtained of the chelating activity of NITA/Mn *via* using different assays of scavenging free radicals. (ABTS, DPPH and metal chelation) assays. Sigma receptors Sigma α-1 receptors are unique; chaperone proteins located primarily in the endoplasmic reticulum (ER) membrane. They are expressed intracellularly in neurons and glia cells and act as the main pharmacochaperones to control neurotransmission by affecting the level of expression of different transporters and receptors. Hence, the cellular receptors of sigma are considered to be involved in the direct potential effects of a lot of drugs. Thus, simulation docking was performed between the Sigma receptor and the novel complex (NITA/Mn).

Result: Based on the molar conductivity value, the (NITA/Mn) complex proved to have a non-electrolytic nature. NITA possess two donation sites through the nitrogen atom of O=C-NH (amide group) and oxygen atom of the O-C=O (ester group) toward Mn (II) metal ion, which was confirmed by IR and UV. SEM and TEM images showed small particles that agglomerated in different shapes. All DFT analysis reinforces that Mn-NITA is energetically more stable and less reactive. The current metal complex NITA/Mn recently chelates with the sigma receptor very effectively via high-forcing docking. The estimated potent scavenging capacities of NITA/Mn confirmed that the capacity of the NITA/Mn complex to scavenge the free radicals of ABTS, DPPH and metal chelation was higher, confirming new potent antioxidant capacities of the synthesized complex. NITA/Mn triggered promising results via a more stable synthesized formula and acted as a potent agent with antioxidant capacities.

Key words: Antioxidant, DFT analysis, Manganese, Metal complex, Nitazoxanide.

INTRODUCTION

Nitazoxanide (NITA) was defined as a broad-spectrum anti-protozoal and anthelmintic agent (Hagras *et al*., 2025; Hagras *et al*., 2023, Amadi *et al*., 2002). NITA is heavily used for the treatment of many protozoa, such as cryptosporidiosis and giardiasis. NITA has been confirmed to possess a great efficiency against several helminthes (Anderson and Curran, 2007; Alonso and Farina, 2020; Colín-Lozano *et al*., 2017). NITA is extremely characterized with its immunomodulatory efficacy (Dupouy-Camet, 2004; Trabattoni *et al*., 2016; Elazar *et al.,* 2009).

Recently, the process of drug discovery has led to novel chemical formulas that have more potent and highly promising activities against many biological pathogens. The main problem facing these novel formulations the poor cellular bioavailability and the poor solubility, which eventually leads to poor simulation (Basavaraj and Betageri, 2014). One of the most potent strategies to overcome this essential complication includes drug encapsulation and this occurs *via* the chelation with metals. It may also lower

[1]Department of Biology, College of Sciences, Taif University, P.O. Box 11099, Taif 21944, Saudi Arabia.

Corresponding Author: Bander Albogami, Department of Biology, College of Sciences, Taif University, P.O. Box 11099, Taif 21944, Saudi Arabia. Email: b.boqami@tu.edu.sa

ORCID: https://orcid.org/0000-0002-2592-8281

How to cite this article: Albogami, B. (2026). Promising Novel Anti-parasitic Drug Nitazoxanide/Mn Metal Complex with its Spectroscopic Characterization, Molecular Docking, DFT Analysis and Assessment of its *in vitro* Antioxidant Activity. *Indian Journal of Animal Research.* **60(9):** 1586-1595. doi: 10.18805/IJAR.BF-2118.

Submitted: 07-03-2026 **Accepted:** 23-05-2026 **Online:** 19-06-2026

any side effects of the original drug and elevate and enhance the stability and the chemical absorbance of the original drug (Sharfalddin *et al*., 2021 and 2023).

Additionally, the used metals in chelation can elevate the cellular penetration of the drug complex *via* enhancing and elevation of its cellular penetration permeability (Kontoghiorghes, 2020). For example, Cu^{+2} ions elevate the new properties of metformin to possess antidiabetic and anticancer capacities (Babak and Ahn, 2021; Müller *et al*., 2018).

Manganese (Mn) plays a crucial role in alleviating oxidative stress through its antioxidant properties. It acts as a cofactor for several enzymes, including Mn SOD which is involved in the detoxification of superoxide. Mn's ability to scavenge free radicals and reduce oxidative stress is attributed to its reactive oxygen species (ROS) production. This antioxidant function is essen tial for maintaining homeostasis and preventing cellular damage due to oxidative stress (Ávila *et al*., 2014).

Another example, "Mn /Minocycline formula", which is a formula of metal ligand biological enhancing properties, as it is known that Minocycline is a broad-spectrum antimicrobial and it is considered a unique tetracycline derivative. But with this chelation with Mn, it produced a novel formula that is more effective as an antioxidant and antibacterial with expected high, potentially significant biological effects (Jastaniah *et al*., 2025).

Sigma receptors are widespread in the C.N.S and multiple tissues. Alpha sigma receptor consists of (σ1R) and (σ2R) and is expressed in numerous regions of the brain. The sigma receptor plays a more diverse role in cellular signaling, apoptosis and metabolic regulation. σ1Rs are intracellular receptors acting as chaperone proteins that modulate Ca^{2+} signaling via the IP3 receptor. The σ1R receptor, at the mitochondrial-associated endoplasmic reticulum membrane, is responsible for mitochondrial metabolic regulation and promotes mitochondrial energy depletion and apoptosis (Rousseaux and Greene, 2016).

There is an emerging indirect relationship between sigma receptors (particularly the sigma-1α receptor) and parasitic infections, primarily through modulation of the host immune response and inflammatory pathways rather than direct binding to the parasite itself. Recently, sigma-1 receptors act as intracellular chaperones, managing endoplasmic reticulum stress and modulating neuroinflammation, which is crucial during parasitic invasions (Tsai *et al*., 2009). Sigma-1 receptors are expressed in immune cells and can regulate the inflammatory response triggered by parasitic infection. Activation of sigma-1 receptors has been shown to reduce inflammatory cytokines in pathological conditions (Tsai *et al*., 2009).

Therefore, in this study, a NITA-based Mn (II) compound was fully synthesized and chemically characterized. Free radical-scavenging *in vitro* biological assays (ABTS, DPPH and metal chelation), besides molecular docking, were used to examine the antioxidant activity and docking efficacy with the sigma receptor for alleviation of both oxidative injury and inflammatory series using this novel complex, respectively.

MATERIALS AND METHODS

Chemicals

Nitazoxanide (NITA) was purchased from a national pharmaceutical company, $MnCl_2$ salt was of pure grade and procured from Sigma-Aldrich Chemical Company.

Synthesis of manganese (Mn) nitazoxanide complex

Solid manganese nitazoxanide was prepared by mixing nitazoxanide (2 mmol, 0.614 g) in 30 mL of methanol as a solvent with (1 mmol) manganese chloride salt: in 20 mL of methanol. The reaction mixture was refluxed for 3 hr. The solid compound was filtered, washed with methanol and then dried under a vacuum over $CaCl_2$.

Chemical characterization methods

A Perkin Elmer CHN 2400 Elemental Analyzer (USA) was used to examine the amounts of C, H and N. The manganese (Mn) compound's electrolytic or non-electrolytic properties were tested using the Jenway 4010 conductivity meter. Infrared spectra in the 4000-400 cm^{-1} spectral range were obtained using a Bruker FT-IR spectrometer. UV-Vis spectra in DMSO between 800 and 200 nm were measured using the UV2 Unicam UV-Vis Spectrophotometer.

Magnetic moments were calculated using Sherwood Scientific's Magnetic Susceptibility Balance. SEM images captured using the Quanta FEG 250 device.

TEM is utilized to explain structural and chemical properties in the nanoscale range through the imaging and diffraction of nanoscale materials. JEOL 100s microscopes were used for TEM studies.

Molecular docking

Molecular docking simulations were performed using AutoDock Vina (Trott and Olson, 2010). Grid boxes were configured to encompass the functional domains. The default exhaustiveness setting was used to ensure adequate conformational sampling.

HOMO-LUMO analysis

Density functional theory (DFT) calculations were performed to estimate the electronic properties and molecular stability or reactivity of Mn-NITA complex neutral singlet ground state, excluding solvent and charge effects. Geometry optimizations and frontier molecular orbital (FMO) analyses were carried out using the B3LYP functional with the 6-311G* (d,p) basis set in the ORCA software package. Molecular visualizations were generated using Avogadro and iBoView. Ionization potential (IP) and electron affinity (EA) were approximated from the negative of the HOMO and LUMO energies, respectively, while electronegativity (χ), electronic chemical potential (μ), chemical hardness (η), softness (S) and electrophilicity index (ω) were derived from

standard conceptual DFT equations. The calculated descriptors, including HOMO-LUMO gap (ΔE), IP, EA, χ, μ, η, S and ω, were used to evaluate the stability and reactivity of each compound, with results summarized in Table 1.

IR analysis

Infrared (IR) spectral analysis of Mn-NITA complex was performed using Density Functional Theory (DFT) at the B3LYP/6-311G*(d,p) level of theory. All calculations were conducted in the neutral singlet ground state without solvent effects. Frequency calculations were carried out to obtain vibrational wavenumbers and intensities, ensuring that no imaginary frequencies were present, thereby confirming the optimized structures as true minima. The simulated spectra were generated using the ORCA quantum chemistry package and visualization was performed with Avogadro and iBoView. Vibrational assignments were made by analyzing the characteristic regions of the spectra, with stretching, bending and deformation modes identified according to their typical frequency ranges.

Raman activity calculations

Raman vibrational properties of Mn-NITA complex computed using density functional theory (DFT). Geometry optimization was initially performed at the selected DFT level (*e.g.*, B3LYP/6-31G (d,p) or your chosen functional/basis set), followed by a full harmonic frequency calculation to obtain vibrational normal modes. Raman activities were calculated from the derivatives of the polarizability tensor with respect to each normal coordinate, as implemented in the quantum chemical package employed for the study. No imaginary frequencies were observed, confirming that the optimised structures correspond to true minima on the potential energy surface. Each Raman-active vibrational mode was then converted into predicted Raman intensities.

Potential energy surface (PES) scanning

The conformational space of Mn-NITA complex was explored through a two-dimensional potential energy surface (PES) scan. Selected dihedral angles or structural coordinates (SC1 and SC2) were systematically varied in defined increments (commonly 10° or 15°), while all remaining internal coordinates were allowed to relax during constrained optimization. For each point on the PES grid, a restricted geometry optimization was performed at the same DFT level used for equilibrium structure determination (*e.g.*, B3LYP/6-311G*(d,p), ensuring consistency across all computed energies. The total electronic energy at each grid point was recorded in atomic units (a.u.) and the resulting dataset was used to generate three-dimensional surface plots and corresponding contour maps. These visualizations allowed identification of energy minima, transition regions and conformational energy barriers. All calculations were conducted without imposing symmetry constraints and convergence thresholds followed default tight optimization settings to ensure numerical stability. The PES surfaces were rendered using scientific plotting software, with energy differences plotted relative to the global minimum to facilitate comparison of conformational stabilities.

Assessment of the antioxidant capacity

Assay of ABTS

Antioxidant activity of NITA and its (Mn) metal ion complex was performed according to Arnao *et al*. (2001) and Elkholy *et al*. (2023). ABTS reagent was dissolved in dis.H_2O. The previously prepared solution was added to $K_2S_2O_8$ and then it was left in the dark for about one day and further procedures. 3 replicates were approved for obtaining the results. The decline in ABTS absorbance was measured at ~734 nm. The results were recorded using a microplate reader, BMG LABTECH®-FLUOstar Omega microplate reader (Ortenberg, Germany).

Linearity of trolox in ABTS assay

Results of the samples are presented as μg TE/mg sample using the linear regression equation extracted from the following calibration curve (linear dose-inhibition curve of Trolox) (Fig 1).

DPPH assay

The antioxidant activity of NITA and its metal complex with (Mn) was measured by using DPPH (2,2-diphenyl-1-picryl-hydrazyl-hydrate) free radical assay (Boly *et al*., 2016 and Elkholy *et al*., 2023). The reactions were incubated for 30 min at 37°C in the dark. 3 replicates were approved for obtaining the results. The resulting reduction in DPPH colour intensity was measured at ~540 nm. The results were recorded using a microplate reader, BMG LABTECH®-FLUOstar omega microplate reader (Ortenberg, Germany) as shown in (Fig 2).

Metal chelation assay

Metal chelation assay was carried out according to Santos *et al.* (2017). Freshly prepared $FeSO_4$ was mixed with NITA and its metal complex with (Mn) ion in the sterilized well plates. Then, the addition of ferrozine. Subsequently, the well plate was incubated at 37°C for ~10 min. After incubation, the decline in the colorimetric intensity was immediately measured at ~562 nm (Santos *et al*., 2017 and Elkholy *et al*., 2023). The results were recorded using a microplate reader, BMG LABTECH®-FLUOstar Omega microplate reader (Ortenberg, Germany) (Fig 3).

Statistical analysis

The data were expressed statistically as (Mean±SE). One-way ANOVA and post hoc test were used. Valuation is significant at ($p<0.05$).

RESULTS AND DISCUSSION

Elemental analysis and molar conductance

Manganese nitazoxanide complex is stable and insoluble in water. The molar conductance measured was Λ_m = 18

(Ω^{-1} mol^{-1} cm^{-1}), confirming the non-electrolytic behaviour as confirmed previously in a lot of studies (El-Megharbel *et al*., 2025; AlZahrani *et al*., 2025 and Al-Thubaiti *et al*., 2025). Elemental analyses (C, H and N) of nitazoxanide complex [Mn $(NITA)_2(cl)_2$] confirmed the 1:2 Mn^{+2}: nitazoxanide ratio.

Infrared spectra

IR data for free nitazoxanide and its Mn (II) metal complex which are shown in (Fig 4). By comparing spectrum of IR for nitazoxanide with its Mn^{+2} complex showed that the stretching vibration of NH amide group disappeared upon chelation to Mn (II) complex and shifted to higher frequencies, confirming that the NH amide group is involved in chelation (Ivana *et al*., 2010). The stretching vibration for ester group appeared at 1772 cm^{-1} and 1160 cm^{-1} due to C=O and C-O, respectively.

A shift in C=O carbonyl group value referred to it was involved in the chelation process. The binding effect to the ester oxygen caused the band, which first emerged in nitazoxanide at 1160 cm^{-1}, to move to a lower frequency with low intensity. The nitazoxanide molecule underwent chelation at these primary sites, undergoes blue shift for C=O amide and C=N modes of vibration in the thiazole ring following chelated to the Mn (II) ion.

For IR for the manganese complex there are new bands appeared at 699 cm^{-1} and 530 cm^{-1} range, which are referred to v(M-O) and a new band appeared at 490 cm^{-1}, referred to v(M-N) (Nakamoto, 1970; Bellamy, 1975).

UV-Vis spectra and magnetic measurements

Table 1 show the uv-vis spectra for free NITA and its Mn complex. For nitazoxanide two absorption maxima appeared at 225 and 410 nm. The band appearing at 410 nm is due to $\pi \rightarrow \pi^*$ transitions, while for 225 nm is attributed to $n \rightarrow \pi^*$ transitions. Weak bands at 280 and 240 nm for Manganese (II) complex, due to to $\pi \rightarrow \pi^*$ and $n \rightarrow \pi^*$ transitions. The octahedral planner shape of the [Mn $(NITA)_2(H_2O)_2Cl_2$] complex was validated by the magnetic moment of 5.236 BM for the Mn (II) complex (Cotton *et al*., 1962; Figgis, 1967).

SEM and TEM investigations

SEM image for NITA and its [Mn $(NITA)_2(H_2O)_2Cl_2$] complex Fig 5. A tiny particle size with nano feature products. Using SEM analysis, the surface morphology of NITA and its Mn^{+2} complex was detected. All particles were shown to have a high capacity to form agglomerates with variety of shapes. TEM images for NITA and its Mn^{+2} complex Fig 5 shows a homogenous phase material that confirms the ordered arrangement for NITA metal chelate matrix and its Mn^{+2} complex. A spherical black spot is appeared within nano-range particle sizes.

Molecular docking of NITA/Mn complex with sigma receptor

Sigma receptors are essentially expressed intracellularly in the nervous system, especially the glial cells and mainly regulate the functions of the ion channels. Additionally, sigma receptors mainly reside in (ER) "Endoplasmic Reticulum" and act as pharmacochaperones to modulate neurotransmission *via* different receptors and

Table 1: Uv-Vs spectra.

Compound	$\pi \rightarrow \pi^*$	$n \rightarrow \pi^*$
NITA	410	225
Mn (II)	280	250

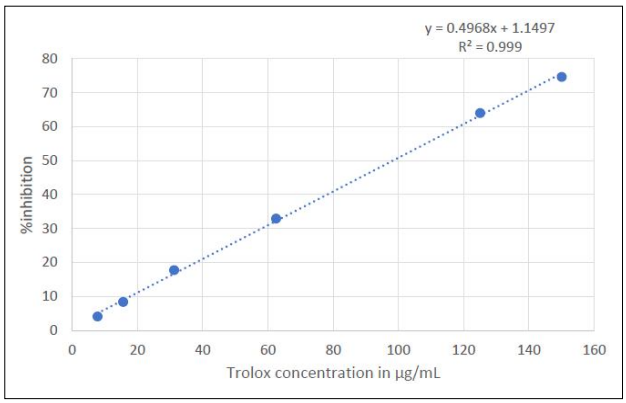

Fig 1: Calibration curve of ABTS assay.

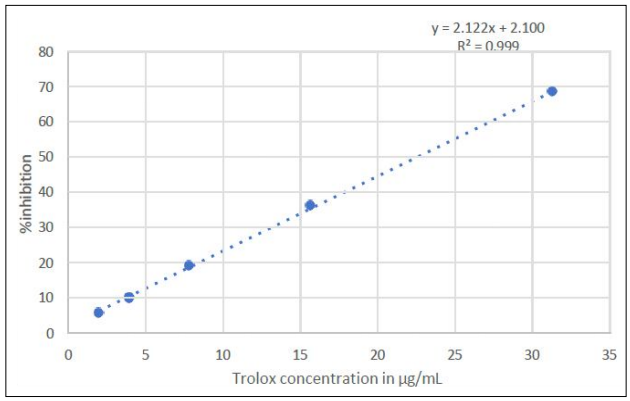

Fig 2: Calibration curve of DPPH assay.

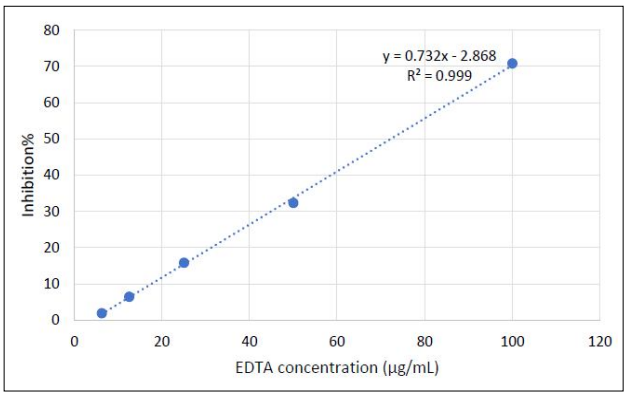

Fig 3: Calibration curve of metal chelation assay.

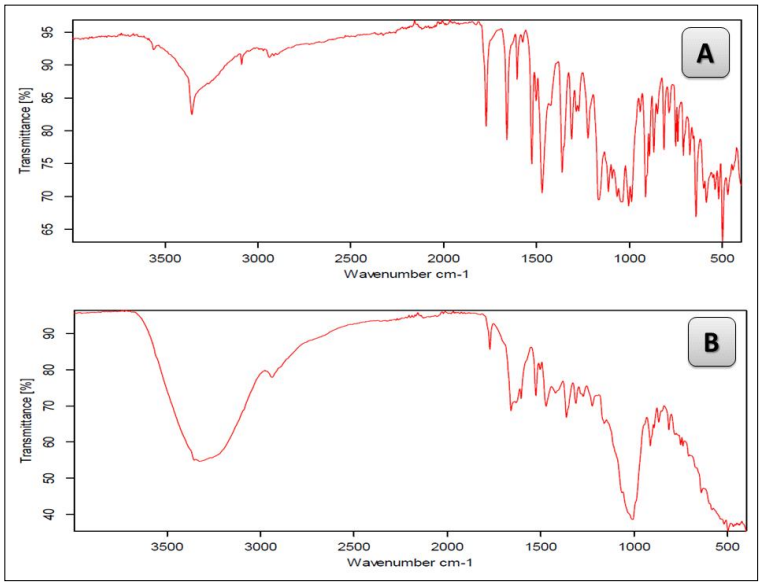

Fig 4: FT-IR of (A) NITA and (B) NITA/Mn.

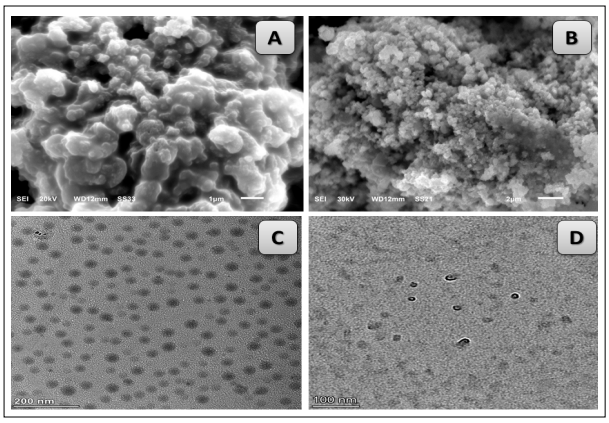

Fig 5: SEM and TEM of (SEM: A: NITA, B: NITA/Mn), (TEM: C: NITA, D: NITA/Mn).

transporters. Thus, sigma receptors are thought to be involved in the effects of many drugs (Liechti *et al*., 2022).

Thus, Sigma α-1 receptors are unique, chaperone proteins located primarily in the endoplasmic reticulum (ER) membrane. They act as ligand-regulated molecular chaperones that modulate ion channels, calcium signaling and neurotransmitter systems, playing crucial roles in neuroprotection, cell survival and psychiatric disorders. Sigma receptors act as intracellular chaperones, often regulating ER stress and calcium flow at the mitochondria-associated ER membrane (MAM). They are highly expressed in the central nervous system and other tissues. While sigma receptor originally thought to be opioid receptors, but the current metal complex NITA/Mn recently chelates with the sigma receptor via recording binding affinity with Med activity and the NITA/Mn complex showed a binding interaction energy ranging from -6.8 to -7.2 kcal/mol for sigma receptor with mean (-6.97) (Table 2) and (Fig 6) which is Med which is a novel result that may open the gate for more prospective studies.

DFT analysis

HOMO-LUMO energy gap calculation and global descriptors

The frontier molecular orbital (FMO) analysis revealed distinct differences in the electronic properties of Mn-NITA complex. Mn-NITA exhibited a HOMO energy of -11.589 eV and a LUMO energy of -5.708 eV, resulting in a relatively large energy gap (ΔE) of 5.881 eV. The larger ΔE value of Mn-NITA indicates greater kinetic stability and lower chemical reactivity. The ionization potential (IP) and electron affinity (EA) further support this trend, with Mn-NITA demonstrating higher IP (11.589 eV), suggesting that Mn-NITA is less prone to electron donation.

The calculated global reactivity descriptors reinforce these observations. Mn-NITA exhibited higher chemical hardness (η = 2.941 eV). Additionally, Mn-NITA (12.72 eV), suggesting a stronger tendency to accept electrons. The chemical potential (μ) and electronegativity (χ) values also reveal that Mn-NITA possesses greater overall electronic stability. Overall, these results suggest that Mn-NITA is comparatively more stable and less reactive, which may influence its interaction behavior in chemical or biological systems, as shown in Table 3 and Fig 7.

IR plot

The IR spectra further confirm the vibrational characteristics of the complex. Strong absorption bands were observed in the 400-1800 cm^{-1} region, with maximum molar absorptivity (ε) values reaching approximately 1100-1200 M^{-1} cm^{-1} for Mn-NITA. Prominent peaks near ~1600-1700 cm^{-1} correspond to azomethine (C=N) stretching vibrations, while bands in the 1000-1300 cm^{-1} region are associated with

C-N and C-O stretching modes. The low-frequency region below 600 cm^{-1} exhibits bands attributed to metal-ligand (M-N and M-Cl) vibrations, confirming successful coordination. Additionally, broad features around ~3400-3550 cm^{-1} indicate O-H stretching vibrations. Notably, Mn-NITA demonstrates a slightly enhanced dipole strength (~1.8 × 10^{-40} $esu^2 \cdot cm^2$), suggesting stronger IR-active transitions in the Mn complex (Fig 8).

Raman activity

The Raman activity spectra of the Mn-NITA complex display prominent vibrational features across the 0-4000 cm^{-1} region. For Mn-NITA complex, intense high-frequency bands were observed in the 3200-3550 cm^{-1} range, corresponding to O-H and N-H stretching vibrations, with maximum intensities approaching ~10-12 arbitrary units and scattering activities nearing ~250 Et /amu. In the fingerprint region (1000-1800 cm^{-1}), distinct strong peaks were recorded around ~1550-1700 cm^{-1}, attributable to C=N and C=S stretching modes. Mn-NITA exhibited comparatively sharper and slightly higher intensity peaks in this region, suggesting stronger metal-ligand coupling. Overall, Mn-NITA complex demonstrates significant Raman activity, with the high-frequency stretching region being the most dominant, as shown in Fig 9.

Potential energy surface (PES) analysis

The three-dimensional potential energy surface (PES) plots reveal the stability landscape of the Mn-NITA complex along the scanned coordinates (SC1). For Mn-NITA, the total energy varies within a narrow range of approximately -438.32 to -438.26 Hartree, showing multiple local minima and maxima, indicative of a rugged energy surface with several accessible conformational states. The deeper

Table 2: Docking score between the novel complex NITA/Mn and the Sigma receptor.

Rank	1	2	3	4	5	6	7	8	9	Mean
Docking score	-7.2	-7.2	-7.1	-7.0	-6.9	-6.9	-6.9	-6.8	-6.8	-6.97

Table 3: The data of chemical reactivity descriptors of the selected four phytochemicals were calculated employing the DFT B3LYP/ 6-311G* basis set method.

Ligand	HOMO (eV)	LUMO (eV)	ΔE (eV)	IP (eV)	EA (eV)	χ (eV)	μ (eV)	η (eV)	S (eV^{-1})	ω (eV)
Mn-NITA	-11.589	-5.708	5.881	11.589	5.708	8.649	-8.649	2.941	0.170	12.72

Here, IP= Ionization potential, EA= Electron affinity, χ= Electronegativity, μ= Electronic potential, η= Chemical hardness, ω= Electrophilicity and S= Chemical softness.

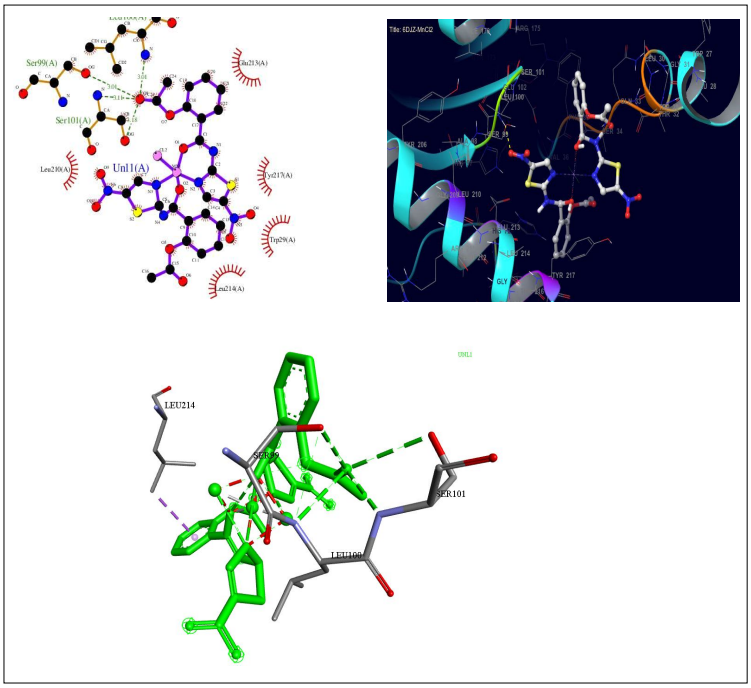

Fig 6: Molecular docking of NITA/Mn with sigma receptor.

minima observed for Mn-NITA suggest greater thermodynamic stability. These findings correlate well with the previously calculated global reactivity descriptors, reinforcing that Mn-NITA is energetically more stable, as shown in Fig 10.

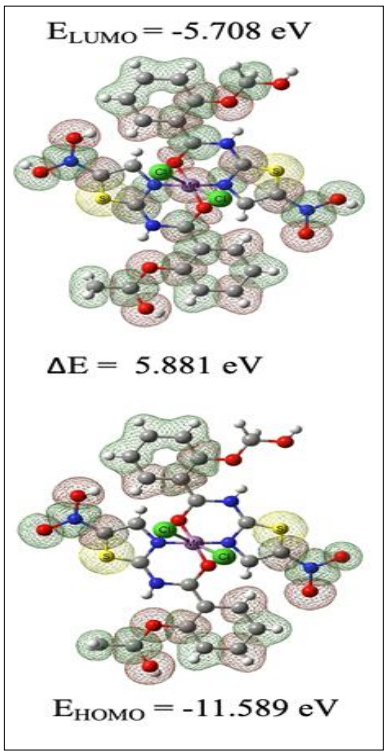

Fig 7: The ground state molecular orbital distribution plots.

Antioxidant capacities of NITA and it's Mn metal complex

The estimated percentages obtained of the chelating activity of NITA/Mn *via* using different assays of scavenging free radicals which are shown in Table 4. The assay of ABTS, Metal chelation and the assay of DPPH were used. The capacity of the NITA and NITA/Mn complex to scavenge the free radicals of ABTS was 230.51, which is more than NITA itself. Meanwhile, the metal chelating activity of NITA/Mn was higher than NITA itself by 72.41% (µM EDTA eq/mg), respectively.

Meanwhile, the scavenging ability of NITA/Mn was also the highest stable via the DPPH radical activity by 26.80 (µM trolox eq/mg). But, the metal complex (NITA/Mn) has a greater chelating capacity by 60.92 (µM trolox eq/mg) than NITA itself (Table 4).

NITA is a commonly used treatment for many types of intestinal protozoa. However, its low solubility is a real barrier for high treatment percentages in many protozoan infections. Thus, there is an urgent need for the development of new drugs to benefit from their tremendous advantages (Hagras *et al*., 2025; Hagras *et al*., 2023).

An innovative scientific trend in the drug delivery models is represented via the new formulation of metal drug complexes in order to overcome a lot of limitations regarding the commercial drugs (Hagras *et al*., 2019; Allam *et al*., 2022).

NPs with a very small size range have high potency to penetrate across the tissues. Consequently, this would increase the permeability of the new drug formulations and decrease the dose of the synthesized drugs. Additionally, these synthesized formulae offer a cost-effective strategy as the nano-encapsulation

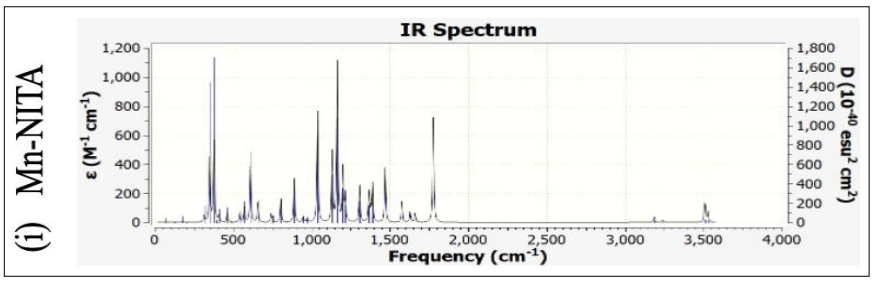

Fig 8: IR plots.

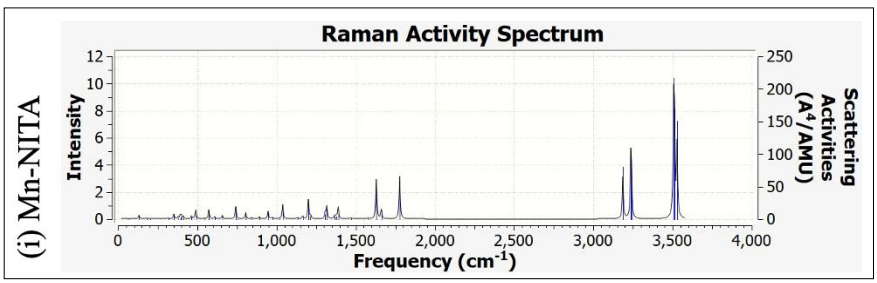

Fig 9: Raman activity.

Table 4: Antioxidant activity of NITA and its metal complex (NITA/Mn).

Test name	ABTS		Metal chelation		DPPH	
Name of the sample	(µM trolox eq/mg)		(µM EDTA eq/mg)		(µM trolox eq/mg)	
	Mean	SD	Mean	SD	Mean	SD
NITA	216.85[b]	10.04	5.42[b]	1.73	26.80[b]	2.14
NITA/Mn	230.51[a]	9.42	19.65[a]	3.56	60.92[a]	8.23

Trolox eq: "Equivalent to the trolox"; Meanwhile, SD: "Standard deviation".

Means within each column category (mean±SE) with different letters are considered as significant, the highest significant value (a) and declining alphabetically.

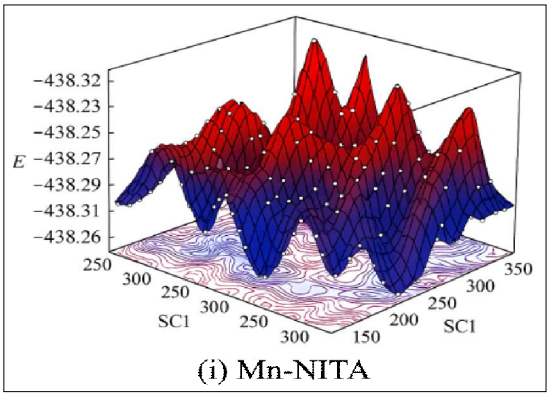

Fig 10: PES analysis.

vehicles' development is almost cheaper (Hagras *et al.,* 2023).

Consequently, the excessive production of the oxidative injury markers due to a lot of parasitic infections is considered as areal and major reason for the incidence of tissue damage (Yan *et al*., 2015). Eventually, the oxidative injury markers of MDA were previously studied (Albogami, 2024 and Albogami, 2025). This oxidative injury is evidenced by the highest MDA levels in the parasitically infected groups. This observation reinforced the novel findings of the current study, which confirmed the antioxidant capacities of the novel complex NITA/Mn over the NITA drug only *via in vitro* antioxidant assays ABTS, DPPH and metal chelation.

Interestingly, the current findings are in great accordance with the study of Hagras *et al*. (2025), who proved that treated groups with NITA-loaded ZnO exhibited a reduction in the estimated oxidative biomarkers, which greatly confirmed the novel concept of the current study *via* the effectiveness of the novel synthesized complex NITA/MN *via* the high *in vitro* antioxidant capacities. These findings are essentially consistent with (Ashour *et al*., 2016; Nagajyothi *et al*., 2015) previous studies, which focused on NITA loaded with ZnO NPs effects in mitigating and declining the oxidative injury due to the parasitic infections.

This surprising decline in the oxidative markers after treatment with NITA new formulations further reinforces the therapeutic benefits of the novel metal complex formula in alleviating the oxidative injury markers associated with parasitic infections, which is in accordance with the previous potent effects of NITA as reported by (Hemphill *et al*., 2006).

The main aim of the current study was to synthesize a nano-sized novel formula of NITA/Mn to enhance its biological actions *via* measurement of the antioxidant capacities *in vitro* and DFT analysis of the utilized novel drug, which confirmed its high energy stability. The nano-formula was synthesized and characterized based in my knowledge for the 1st time as a potent antioxidant *via in vitro* antioxidant assay. The results of the NITA/Mn characterization denoted that it lies in the nano-sized range. This smaller particle's size saves high surface area as compared to the volume and eventually leads to higher penetration across the cellular membranes (Melk *et al*., 2021).

FTIR spectroscopy exhibited peaks that are attributed to (MnO stretching) the metal-oxygen vibration mode, while the clear shift that appeared in the FT-IR peaks indicates a high success of NITA/Mn as previously confirmed (Sawant *et al*., 2018).

Simulation docking with sigma receptor and DFT analysis revealed that NITA/Mn metal complex exhibited a Med docking force with Med energy stability. This is usually preferable as it offers a sufficient drug amount across the body tissues (El-Wakil *et al*., 2023).

There is an emerging indirect relationship between sigma receptors (particularly the sigma-1α receptor) and parasitic infections and inflammatory pathways, rather than direct binding to the parasite itself. Recently, sigma-1 receptors act as intracellular chaperones, managing endoplasmic reticulum stress and modulating neuroinflammation, which is crucial during parasitic invasions. This is in agreement with the current concept regarding a NITA-based Mn (II) compound with its activity in docking with this receptor and concurrently its potent antioxidant activities.

The mechanism of action of NITA is represented by inhibiting the pyruvate ferredoxin oxido-reductase enzyme, which can alter the parasitic metabolism, especially the respiratory system, besides causing a lot of cellular membrane lesions (Hagras *et al*., 2023). Despite the safe NITA nature in general, it still has decreased efficacy due mainly to its poor solubility as previously mentioned. Even NITA/Mn revealed the highest significant drug stability, which offered Med benefits *via* improving the drug solubility

that can effectively enhance in prospective *in vivo* studies, the drug permeability and the efficacy.

CONCLUSION

NTZ/Mn complex was synthesized and it's *in vitro* antioxidant activity was assessed. The complex proved to have a non-electrolytic nature. Its chemical structure was confirmed by IR and UV. SEM and TEM images showed small particles that agglomerated in different shapes. All DFT analysis reinforces that Mn-NITA is energetically more stable and less reactive. NITA/Mn chelates with the sigma receptor very effectively *via* high-forcing docking. The estimated scavenging capacities of NITA/Mn confirmed the potent capacity of NITA/Mn complex to scavenge the free radicals of ABTS, DPPH and metal chelation, confirming new potent antioxidant capacities of the synthesized complex.

ACKNOWLEDGEMENT

The author would like to acknowledge the Deanship of Graduate Studies and Scientific Research, Taif University, for funding this work.

Disclaimers

The author is responsible for the accuracy and completeness of the information provided.

Conflict of interest

The author declares that there is no conflict of interest regarding the publication of this article. No funding or sponsorship influenced the design of the study, data collection, analysis, decision to publish, or preparation of the manuscript.

REFERENCES

Albogami, B. (2024). Research article ellagic acid ameliorates hepatic functions against the hepatic alterations induced by nitazoxanide (Antiprotozoal drug) in male rats. *Int. J. Pharmacol.* **20:** 1198-1208.

Albogami, B. (2025). Efficacy and promising ameliorative effect of crocin against *Cryptosporidium parvum* with colon ultrastructure examination in male rats. *International Journal of Pharmacology.* **21(1):** 103-112.

Allam, A.F., Hagras, N.A.E., Farag, H.F., Osman, M.M., Shalaby, T.I., Kazem, A.H. *et al.* (2022). Remarkable histopathological improvement of experimental toxoplasmosis after receiving spiramycin-chitosan nanoparticles formulation. *J. Parasit. Dis*. **46(1):** 166-177.

Alonso, D.F. and Farina, H.G. (2020). Repurposing of host-based therapeutic agents for the treatment of coronavirus disease 2019 (COVID-19): A link between antiviral and anticancer mechanisms? *International Journal of Antimicrobial Agents*. **56(3):** 106125.

Al-Thubaiti, E.H., Hamza, R.Z., Alaidaroos, B.A., Al-Gheffari, H.K., Albaqami, N.M. and El-Megharbel, S.M. (2025). Chemical characterization of pollen grains ethanolic extract (PGE) with evaluation of its potent antioxidant, antibacterial and anti-cancer activities against hepatocellular carcinoma (HepG2). *Indian Journal of Animal Research.* **59(10):** 1653-1662. doi: 10.18805/IJAR.BF-1953.

AlZahrani, S.S., El-Megharbel, S.M., Al-Thubaiti, E.H., Alghamdi, M.A., Hassoubah, S.A., Qattan, S.Y.A., Alaidaroos, B.A., Albqami, N.M., AL-Harbi, M.S. and Hamza, R.Z. (2025). Chemical and spectroscopic characterization of novel dexamethasone/zn complex as a potent antioxidant and antibacterial agent. *Indian Journal of Animal Research*. **59(8):** 1329-1340. doi: 10.18805/IJAR.BF-1939.

Amadi, B., Mwiya, M, Musuku, J., Watuka, A., Sianongo, S., Ayoub, A. and Kelly, P. (2002). Effect of nitazoxanide on morbidity and mortality in zambian children with cryptosporidiosis: A randomised controlled trial. *Lancet.* **360(9343):** 1375-1380.

Anderson, V.R. and Curran, M.P. (2007). Nitazoxanide. *Drugs*. **67:** 1947-1967.

Arnao, M.B., Cano, A. and Acosta, M. (2001). The hydrophilic and lipophilic contributions to total antioxidant activity. *Food Chemistry.* **73:** 239-244.

Ashour, D.S., Abou Rayia, D.M., Saad, A.E. and El-Bakary, R.H. (2016). Nitazoxanide anthelmintic activity against the enteral and parenteral phases of trichinellosis in experimentally infected rats. *Exp. Parasitol.* **170:** 28-35.

Ávila, D.S., Farina, M., Teixeira da Rocha, J.B. and Aschner, M. (2014). In: Manganese in Health and Disease, [Costa, L. and Aschner, M. (eds)]. *The Royal Society of Chemistry*. **8:** 199-220.

Babak, M.V. and Ahn, D. (2021). Modulation of intracellular copper levels as the mechanism of action of anticancer copper complexes: Clinical relevance. *Biomedicines.* **9:** 852.

Basavaraj, S. and Betageri, G.V. (2014). Can formulation and drug delivery reduce attrition during drug discovery and development-review of feasibility, benefits and challenges. *Acta Pharm. Sin. B*. **4(1):** 3-17.

Bellamy, L.J. (1975). The Infrared Spectra of Complex Molecules, Chapman and Hall, London, UK.

Boly, R., Lamkami, T., Lompo, M., Dubois, J. and Guissou, I. (2016). DPPH free radical scavenging activity of two extracts from *Agelanthus sosoneifolius* (*Loranthaceae*) leaves. *International Journal of Toxicological and Pharmacological Research.* **8(1):** 29-34.

Colín-Lozano, I. León-Rivera, Chan-Bacab, M.J., Ortega-Morales, B.O., MooPuc, R., López-Guerrero, V., Hernández-Núñez, E., Argüello-Garcia, R., Scior, T. and Barbosa-Cabrera, E. (2017). Synthesis, *in vitro* and *in vivo* giardicidal activity of nitrothiazole-NSAID chimeras displaying broad antiprotozoal spectrum. *Bioorganic* and *Medicinal Chemistry Letters*. **27:** 3490-3494.

Cotton, F.A., Goodgame, D.M.L. and Goodgame, M. (1962). Absorption spectra and electronic structures of some tetrahedral manganese (ii) complexes. *J. Am. Chem. Soc.* **84(2):** 167.

Dupouy-Camet, J. (2004). New drugs for the treatment of human parasitic protozoa. *Parassitologia.* **46(1-2):** 81-84. PMID: 15305692.

Elazar, M., Liu, M., McKenna, S.A., Liu, P., Gehrig, E.A., Puglisi, J.D., agnol, J.F. and Glenn, J.S. (2009). The anti-hepatitis C agent nitazoxanide induces phosphorylation of eukaryotic initiation factor 2a *via* protein kinase activated by double-stranded RNA. *Gastroenterology*. **137:** 1827-1835.

Elkholy, N.S., Hariri, M.L.M., Mohammed, H.S. *et al.* (2023). Lutein and β-carotene characterization in free and nanodispersion forms in terms of antioxidant activity and cytotoxicity. *J. Pharm. Innov.* **18:** 1727-1744.

El-Megharbel, S.M., Albogami, B., Alaidaroos, B.A., Al-Gheffari, H.K., Albaqami, N.M., Albaqami, J.J., AL-Harbi, M.S. and Hamza, R.Z. (2025). Spectroscopic analysis of copper minocycline novel complex and evaluation of its potent antibacterial, antioxidant and anti-breast cancer (MCF-7) properties. *Indian Journal of Animal Research.* **59(7):** 1120-1130. doi: 10.18805/IJAR.BF-1948.

El-Wakil, E.S., Khodear, G.A.M., Ahmed, H.E.S., Ibrahim, G.I.K., Hegab, F. and Abdo, S.M. (2023). Therapeutic efficacy of albendazole and berberine loaded on bovine serum albumin nanoparticles on intestinal and muscular phases of experimental trichinellosis. *Acta. Trop.* **241:** 106896.

Figgis, B.N. (1967). "Introduction to Ligand Fields", Interscience Publishers, John Wiley and Sons, New York. pp. 285.

Hagras, N.A., Hegab, F., Atta, S., Gadallah, R.A., Elsayed, Y. and Khodear, G.A.M. (2025). Promising therapeutic efficacy of nitazoxanid-loaded zinc oxide nano-formula against intestinal and muscular phases of experimental trichinellosis. *Plos Negl. Trop. Dis.* **19(7):** e0013239.

Hagras, N.A.E., Allam, A.F., Farag, H.F., Osman, M.M., Shalaby, T.I., Fawzy, H., Mogahed, N.M. *et al*. (2019). Successful treatment of acute experimental toxoplasmosis by spiramycin-loaded chitosan nanoparticles. *Exp. Parasitol.* **204:** 107717.

Hagras, N.A.E., Makled, S., Sheta, E., El-Hawary, M.A. and Mogahed, N.M.F.H. (2023). Potent efficiency of the novel nitazoxanide-loaded nanostructured lipid carriers against experimental cyclosporiasis. *PLoS Negl. Trop. Dis.* **17(12):** e0011845.

Hemphill, J., Mueller, M. and Esposito. (2006). Nitazoxanide, a broad-spectrum thiazolide anti-infective agent for the treatment of gastrointestinal infections. *Expert Opinion on Pharmacotherapy*. **7:** 953-964.

Ivana, A.J., Zoran, V.S., Enis, S.D. and Jovan, M.N. (2010). New hybrid properties of TiO(2) nanoparticles surface modified with catecholate type ligands. *J. Nano Scale Res. Lett.* **5:** 81-88.

Jastaniah, S.D., El-Megharbel, S.M., Alsolami, K., Alsulami, M.N., Albaqami, N.M., Albogami, B. and Hamza, R.Z. (2025). Spectroscopic and chemical characterization of the novel minocycline/Mn complex with evaluation of its *in vitro* potent antioxidant activity and high antibacterial effect against *Escherichia coli* (ATCC 8739), *Bacillus subtilis* (ATCC6633), *Staphylococcus aureus* (ATCC 6538) and *Klebsiella pneumonia* (ATCC 13883). *Polyhedron.* **265:** 117287.

Kontoghiorghes, G.J. (2020). Advances on chelation and chelator metal complexes in medicine. *International Journal of Molecular Sciences*. **21(7):** 2499.

Liechti, M.E., Simmler, L.D., Sitte, H.H. and Luethi, D. (2022). Chapter 4-Pharmacological profiling of novel psychoactive substances. Novel Psychoactive Substances (2nd Edition) Classification, Pharmacology and Toxicology. pp. 109-130.

Melk, M.M., El-Hawary, S.S., Melek, F.R., Saleh, D.O., Ali, O.M., El Raey, M.A. *et al.* (2021). Antiviral activity of zinc oxide nanoparticles mediated by *Plumbago indica* L. extract against herpes simplex virus type 1 (HSV-1). *Int. J. Nanomedicine.* **16:** 8221-8233.

Müller, S., Versini, A., Sindikubwabo, F., Belthier, G., Niyomchon, S., Pannequin, J., Grimaud, L., Cañeque, T. and Rodriguez, R. (2018). Metformin reveals a mitochondrial copper addiction of mesenchymal cancer cells. *Plos One*. **13:** e0206764.

Nagajyothi, P.C., Cha, S.J., Yang, I.J., Sreekanth, T.V.M., Kim, K.J. and Shin, H.M. (2015). Antioxidant and anti-inflammatory activities of zinc oxide nanoparticles synthesized using *Polygala tenuifolia* root extract. *J. Photochem Photobiol B.* **146:** 10-17.

Nakamoto, K. (1970). Infrared Spectra of Inorganic and Coordination Compounds 2nd Edition. Wiley Interscience, John Wiley and Sons, New York, NY, USA.

Rousseaux, C.G. and Greene, S.F. (2016). Sigma receptors [σRs]: Biology in normal and diseased states. *J. Recept Signal Transduct Res.* **36(4):** 327-388.

Santos, J.S., Brizola, V.R.A. and Granato, D. (2017). High-throughput assay comparison and standardization for metal chelating capacity screening: A proposal and application. *Food Chemistry*. **214:** 515-522.

Sawant, V.J. and Bamane, S.R. (2018). PEG-beta-cyclodextrin functionalized zinc oxide nanoparticles show cell imaging with high drug payload and sustained pH responsive delivery of curcumin in to MCF-7 cells. *J. Drug Deliv Sci. Technol.* **1(43):** 397-408.

Sharfalddin, A.A., Al-Younis, I.M., Emwas, A.H. and Jaremko, M. (2023). Investigating the biological potency of nitazoxanide-based Cu(II), Ni(II) and Zn(II) complexes synthesis, characterization and anti-COVID-19, antioxidant, antibacterial and anticancer activities. *Molecules.* **28:** 6126.

Sharfalddin, A.A., Emwas, A., Jaremko, M. and Hussien, M.A. (2021). Transition metal complexes of 6-mercaptopurine: Characterization, theoreticalcalculation, DNA-binding, molecular docking and anticancer activity. *Appl. Organo. Met Chem*. **35:** e6041.

Trabattoni, D., Gnudi, F., Ibba, S.V., Saulle, I., Agostini, S., Masetti, M. *et al.* (2016). Thiazolides elicit anti-viral innate immunity and reduce HIV replication. *Sci. Rep.* **6:** 27148.

Trott, O. and Olson, A.J. (2010). AutoDock Vina: improving the speed and accuracy of docking with a new scoring function, efficient optimization and multithreading. *J. Comput. Chem.* **31(2):** 455-461.

Tsai, S.Y., Hayashi, T., Mori, T. and Su, T. (2009). Sigma-1 receptor chaperones and diseases. *Cent. Nerv. Syst. Agents. Med. Chem*. **9(3):** 184-189.

Yan, X., Ji, Y., Liu, X. and Suo, X. (2015). Nitric oxide stimulates early egress of Toxoplasma gondii tachyzoites from human foreskin fibroblast cells. *Parasit Vectors*. **13(8):** 420.